

Data and text mining

# ProgPermute: Progressive permutation for a dynamic representation of the robustness of microbiome discoveries

Liangliang Zhang<sup>1,\*</sup>, Yushu Shi<sup>1</sup>, Kim-Anh Do<sup>1</sup>, Christine B. Peterson<sup>1</sup>, Robert R. Jenq<sup>2</sup>

<sup>1</sup>Department of Biostatistics, University of Texas MD Anderson Cancer Center, Houston, Texas, U.S.A.

<sup>2</sup>Department of Genomic Medicine, University of Texas MD Anderson Cancer Center, Houston, Texas, U.S.A.

\*To whom correspondence should be addressed.

Associate Editor: XXXXXXXX

Received on XXXXX; revised on XXXXX; accepted on XXXXX

## Abstract

**Motivation:** The human microbiota has been shown to be linked to health and diseases. Identification of significant features is a critical task in microbiome studies that is complicated by the fact that microbial data are high dimensional and heterogeneous. Masked by the complexity of the data, the problem of separating signal from noise becomes challenging and troublesome. For instance, when performing differential abundance tests, multiple testing adjustments tend to be overconservative, as the probability of a type I error (false positive) increases dramatically with the large numbers of hypotheses. Moreover, the main grouping effect is usually mixed with heterogeneity. These facts can incorrectly lead to the conclusion that there are no differences in the microbiome. Additionally, these methods do not convey the overall association between microbiome and the grouping factor of interest, and do not quantify the robustness of the discoveries and the reliability of the results.

**Results:** We represent the significance identification problem as a dynamic process of separating signals from a randomized background. The signals and noises in this process will converge from fully mixing to clearly separating, if the original data is differential by the grouping factor. We propose the progressive permutation method to achieve this process and show the converging trend. The proposed method progressively permutes the grouping factor labels of microbiome and performs multiple differential abundance tests in each scenario. We compare the signal strength of top hits from the original data with their performance in permutations, and will observe an apparent decreasing trend if these top hits are true positives identified from the data. To help understand the robustness of the discoveries and identify best hits, we develop a user-friendly and efficient RShiny tool. Simulations and applications on real data show that the proposed method can evaluate the overall association between microbiome and the grouping factor, rank the robustness of the discovered microbes, and list the discoveries, their effect sizes, and individual abundances.

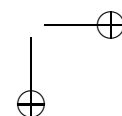
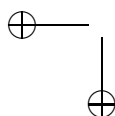
**Availability:** Shiny App is accessible at <https://biostatistics.mdanderson.org/shinyapps/ProgPerm>. Codes and example data are available at <https://github.com/LyonsZhang/ProgPermute>.

**Contact:** liangliangzhang.stat@gmail.com

**Supplementary information:** Supplementary data are available at *Bioinformatics* online.

## 1 Introduction

With the advent of next-generation sequencing technologies to quantify the composition of human microbiome, there have been drastic



increases in the number of microbiome studies and vast improvements in microbiome analysis (Knight *et al.*, 2018). In recent decades, a tremendous amount of evidence has strongly suggested that the human microbiota is becoming a crucial key to understanding human health and physiology (Jie *et al.*, 2017; Vogt *et al.*, 2017; Cani and Jordan, 2018; Wei *et al.*, 2018; Gopalakrishnan *et al.*, 2018; Ong *et al.*, 2018; Riquelme *et al.*, 2019). In practice, identification of microbial biomarkers often requires singling out specific taxa that are differentially abundant between two groups of interest (e.g. treatment vs. control). Differential abundance analysis (Paulson *et al.*, 2013) in this setting, however, is challenging. Because a single sample can produce as many as tens of thousands of distinct sequencing reads. These reads are clustered into operational taxonomic units (OTUs) and mapped to the microbial species according to a reference library. At the same time, the OTUs (can be considered as the lowest level taxa) are routinely aggregated to higher taxonomic levels (phyla, order, class, family, genus, or species). As a result, microbiome data are high dimensional and heterogeneous across samples.

Researchers have adapted classical differential analysis tools developed for RNA sequencing data, such as edgeR (Robinson *et al.*, 2010) and DESeq (Love *et al.*, 2014), to microbiome data, as both data types are essentially read count data. Others proposed methods specially account for the compositional nature of microbiome data, including ANCOM (Mandal *et al.*, 2015) and ALDEx2 (Fernandes *et al.*, 2014). Segata *et al.*, 2011 developed LefSe (Linear discriminant analysis Effect Size) to identify differential taxonomic features between groups by using standard tests for statistical significance. When doing multiple tests, the probability of a Type I error (false positive) increases dramatically as high throughput sequencing data is tested (Goeman and Solari, 2014). Adjustment methods such as the Benjamini-Hochberg procedure will become over-conservative and incorrectly lead to conclusions that there are no differences in the microbiome, because the thresholds of rejecting the null hypothesis for each microbe becomes extremely small as the number of tests increases (Jiang *et al.*, 2017). Although these differential testing methods are able to identify the significance of individual microbiomarkers, they do not evaluate the overall association between the microbiome and the grouping factor. Dimension reduction plots (e.g. PCoA or NMDS) explore the overall associations, but the expected clustering effect may not necessarily be witnessed, because the heterogeneity across samples is high. Therefore, these existing methods can lack power to reach consensus on the robustness of the discoveries and the reliability of the results.

Based on these considerations, we propose a novel method named the progressive permutation. The method represents the significance identification problem as a dynamic process of separating signals from a randomized background. The method progressively permutes the grouping factor labels of microbiome samples and performs differential testing methods (such as a Wilcoxon rank-sum test or a Kruskal-Wallis test) in each scenario. We then compare the signal strength ( $-\log_{10} p$ -values) of top hits from the original data with their performance in permuted data sets. We can observe an apparent decreasing trend if these top hits are true positives identified from the data. We also extend these concepts to a continuous outcome using correlation tests (such as Kendall's tau or Spearman Rank Correlation tests). We have developed this method into a user-friendly and efficient RShiny tool with visualizations, so that the method becomes easy to apply, the results are easy to understand and the analyzing process is well organized. Smirnova *et al.*, 2019 proposed a permutation filtering method to measure the taxa importance by the filtering loss of exclusion of the taxa. The method randomly permutes the labels of taxa and evaluate proportion of total variance loss. Our method permutes the sample labels to regroup them and evaluate the robustness of group differences. The Fragility index is a measure of the robustness of the results of a clinical trial (Walsh *et al.*,

2014; Feinstein, 1990). We propose a similar concept in our progressive permutation to evaluate the robustness of each significant taxa. We validate our method with simulations and applications in real data. We conclude that the proposed method can not only evaluate the overall association between the microbiome and a grouping factor (that might be obscured by heterogeneity), but also single out the significance of individual hits. It achieves the former by measuring the steepness of U-Curve of number of significant hits across permutation scenarios and ranking the Fragility Index of the discovered microbes. It achieves the latter by comparing the p-values of the original data with p-values of the full permuted data. To finalize the results, the RShiny tool lists the discoveries, their effect sizes and individual abundances.

The paper is organized as follows. In Section 2, we include a detailed description of the proposed method. In Section 3, we run simulations, and use U-Curve and fragility index to measure the overall association with the grouping factor and the robustness of microbiome discoveries. In Section 4, we apply the method to real data to test the overall association and identify significant hits. We conclude with a discussion in Section 5.

## 2 Approach

Suppose we collect  $N$  samples across  $p$  variables. The variables are denoted as  $\mathbf{X} = (\mathbf{x}_1, \dots, \mathbf{x}_p)$ , where each  $\mathbf{x}_i$  is an  $N$ -dimensional vector. We aim to identify which variables are differential by the grouping factor of interest with two groups  $\mathbf{g} = (\mathbf{g}^1, \mathbf{g}^2)$ . We denote the grouping labels as  $g_i^1 = 1, i = \{1, \dots, n_1\}$  and  $g_i^2 = 2, i = \{1, \dots, n_2\}$ , where  $n_1 + n_2 = N$ . The hypothesis test performed on each variable is denoted as  $H_j, j = \{1, \dots, p\}$ . The corresponding p-value is denoted as  $p_j, j = \{1, \dots, p\}$ .

We use  $k = \{0, 1, \dots, K\}$  to describe progressive permutation scenarios.  $k = 0$  describes the original data without any permutation.  $K = \min(n_1, n_2)$  is the maximal permutation scenario. The permutation scenario  $k$  is constructed as follows. Each time, we start from the original grouping labels  $\mathbf{g} = (\mathbf{g}^1, \mathbf{g}^2)$ . We randomly draw  $k$  samples from group 1 (sample labels  $\{i_1^1, \dots, i_k^1\} \subseteq \{1, \dots, n_1\}$ ) and  $k$  samples from group 2 (sample labels  $\{i_1^2, \dots, i_k^2\} \subseteq \{1, \dots, n_2\}$ ), and then exchange their grouping labels, meaning that  $g_i^1 = 2, i = \{i_1^1, \dots, i_k^1\}$  and  $g_i^2 = 1, i = \{i_1^2, \dots, i_k^2\}$ . In the  $k$ -th permutation scenario, we have  $\binom{n_1}{k} \binom{n_2}{k}$  choices. The number of choices  $\binom{n_1}{k} \binom{n_2}{k}$  approaches its maximum, when  $k$  equals the closest integer greater than  $K_m = \frac{n_1 n_2 - 1}{n_1 + n_2 + 2}$ . If  $n_1 = n_2 = n$ , then  $K_m = \frac{n-1}{2}$ . Adding up the choices of all the scenarios, we get the following equation

$$\sum_{k=0}^K \binom{n_1}{k} \binom{n_2}{k} = \binom{N}{K}.$$

The above equation can be derived from Vandermonde's convolution identity for binomial coefficients. The details are shown in Section S1 of Supplementary material. The left side lists all the progressive permutation scenarios which are disjoint meaning that grouping labels are distinct between scenarios. The right side lists all possible combinations when you group  $N$  samples into two subgroups with  $n_1$  and  $n_2$  samples respectively. With the increase of  $k$ , the two groups are mixing more with each other. In other words, among all the grouping assignments at random, the permuted assignments more similar to the original data (the observed grouping factor) would differentiate the two groups more than the less similar ones, if the variables were strongly associated with the observed grouping factor.

Given the properties, next we introduce how to use the progressive permutation results. For each draw in every scenario  $k$ , we perform  $p$  independent tests and calculate all the  $p$ -values. We can obtain the number of significant taxa as  $\text{nsig}(k) = \sum_{j=1}^p I_{p_j(k) \leq \alpha}$ , where  $\alpha$  is

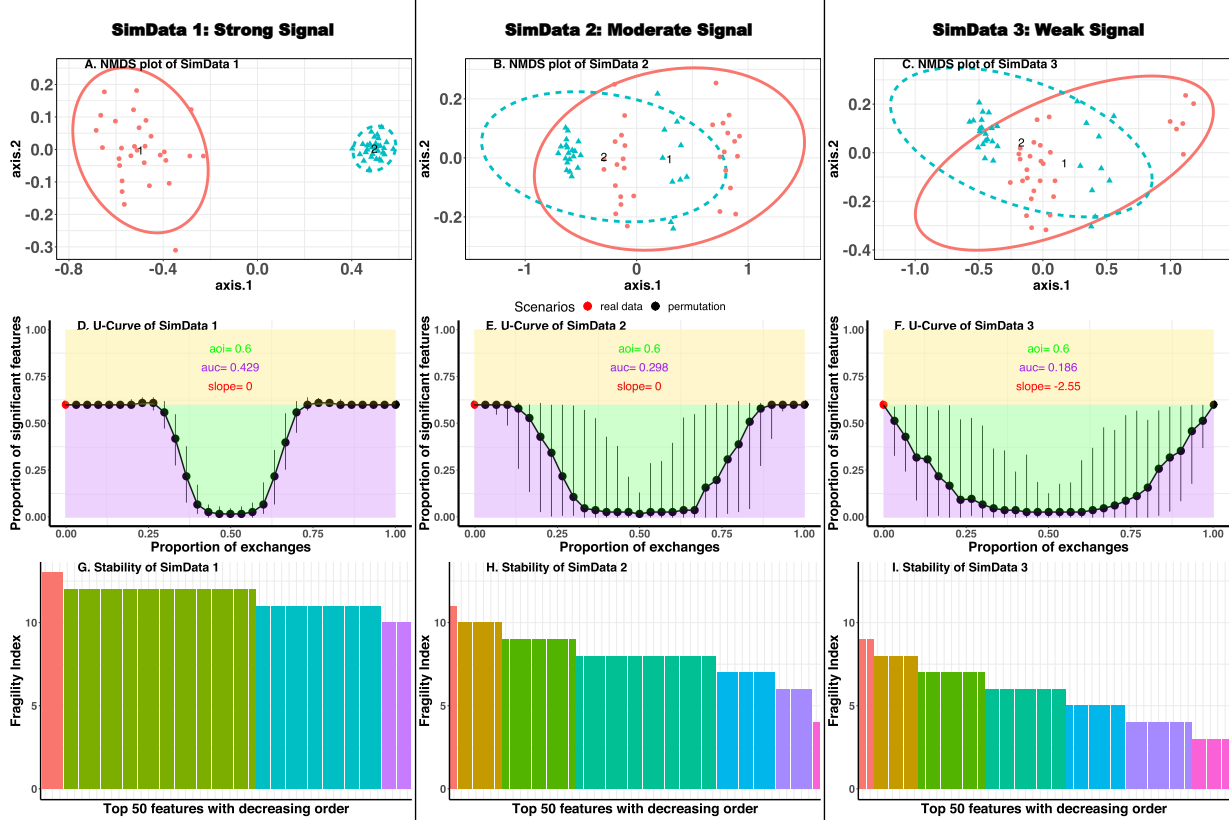


**Fig. 1.** Result comparisons of three simulated data with different levels of confounding effects. The first row (A,B C) shows the NMDS plot using the Bray-Curtis distance. The second row (D, E, F) shows the U-Curve of proportion of significant features. "aoi" is short for "area of interest", which denotes the proportion of significant features out of all the features (area of green plus purple). "auc" is short for "area of curve", which denotes the area under the U-Curve (area of purple). "slope" denotes the slope of the red point. The red point denotes the real data. The third row (G, H, I) shows the fragility index. To save space, the legend listing the names of the 50 features are omitted.

the prespecified significance level. We expect to see the lowest  $\text{nsig}(k)$  in the fully mixing scenario  $K_f$ , where  $K_f \in \{0, 1, \dots, K\}$ . The number of significant hits  $\text{nsig}(k)$  decreases with the proportion of permutations  $\frac{k}{K}$ , when  $k \leq K_f$ .  $\text{nsig}(k)$  increases with the proportion of permutations  $\frac{k}{K}$ , when  $k \geq K_f$ . We will provide an analytical form of  $K_f$  with simplistic setups in Section 5. In the next section, we will see the U-Curve shape of number of significant taxa across permutation scenarios. As the shape of U-Curve measures how differential the microbiome compositions are between the two groups, we potentially can use the U-Curve as a global statistic to measure the overall association between microbiome compositions and the grouping factor of interest.

The fragility index of  $j$ th variable at permutation scenario  $k$  is defined as  $\text{FI}_j = \min_k (p_j(k) > \alpha)$ . In other words, fragility index of a variable is the minimum number of permutation steps that would change the variable's significance into nonsignificance. The larger the fragility index is, the more stable the identified taxa are. Therefore, we can rank the importance of the taxa by their fragility indices.

### 3 Simulations

In this section, we simulate three data sets with different levels of heterogeneity. Then we compare the performance of our progressive permutation method on these data.

We follow the same simulation setup used by Hawinkel *et al.*, 2019. We simulate the OTU counts as random samples drawn from a negative binomial distribution  $X_j \sim \mathcal{F}(\mu, \kappa)$ ,  $j = 1, \dots, p$ .  $\kappa$  is called the

dispersion parameter, as the variance of  $X_j$  is  $\mu + \frac{\mu^2}{\kappa}$ . To simulate the dependence between OTUs, we use the Gaussian copula (Owen, 2013) to combine the correlation structure  $\mathbf{R}$  with the negative binomial distributions. Here are the simulation steps. First, we draw Gaussian samples of  $Z \sim \mathcal{N}(0, \mathbf{R})$ . Second, we obtain the negative binomial samples  $X_j = F_j^{-1}(\Phi(Z_j))$ . Third, we obtain the compositions by dividing each element  $X_{ij}$  by a constant.

We generate three simulation data sets, which are denoted as SimData 1, SimData 2 and SimData 3. They have the same sample size  $N = 60$  and same number of variables  $p = 100$ . The 60 samples differ abundantly between Group 1 (30 samples) and Group 2 (30 samples). We denote data of Group 1 as  $D_1$  and data of Group 2 as  $D_2$ . For the 100 variables, we define the proportion of significant features to be 0.6, which implies that 60 variables are significant. To construct confounding effects, we create the second source of difference by splitting Group 1 into two subgroups of samples, which are denoted as  $D_{11}$  and  $D_{12}$ . In the same way, we split Group 2 into two subgroups of samples, which are denoted as  $D_{21}$  and  $D_{22}$ . The grouping factor of interest  $y$  is  $[1, \dots, 1, 2, \dots, 2]$ .

We describe the data generation as follows. We use  $(m)_c$  to denote a sequence containing  $c$  number of  $m$ .  $\text{RN}(\mu_0, \sigma_0)$  describes the random number drawn from normal distribution with mean  $\mu_0$  and variance  $\sigma_0$ . We define the correlation structure as  $R_{ij} = \rho^{i-j}$ .  $\rho$  is set up as 0.5. Zero-Inflation is one of the main characteristics of microbiome data. Note that  $\mu$  controls the magnitude of each variable and number of zeros in each sample. The distribution of zeros across samples and variables of SimData 1, SimData 2 and SimData 3 is comparable to the distribution of zeros

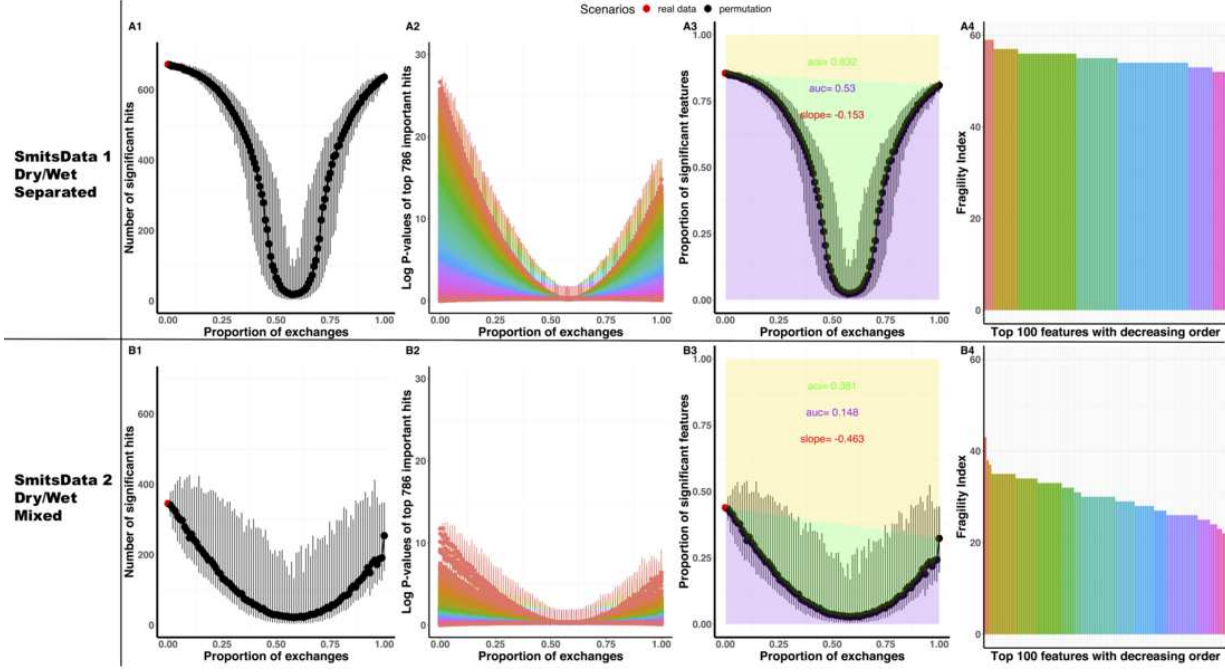


**Fig. 2.** Result comparisons of regrouped data SmitsData 1 (A1-A4) and SmitsData 2 (B1-B4) with different levels of confounding effects. A1 and B1 plot the U-Curve of number of significant hits. In A2 and B2, we rank the significance of the 786 features, and then plot their  $-\log_{10} p$ -values with the same order across permutation scenarios. A3 and B3 plot the U-Curve of proportion of significant hits. A4 and B4 plots the fragility index of the top 100 features with a decreasing order. To save space, the legend listing the names of the 100 features are omitted.

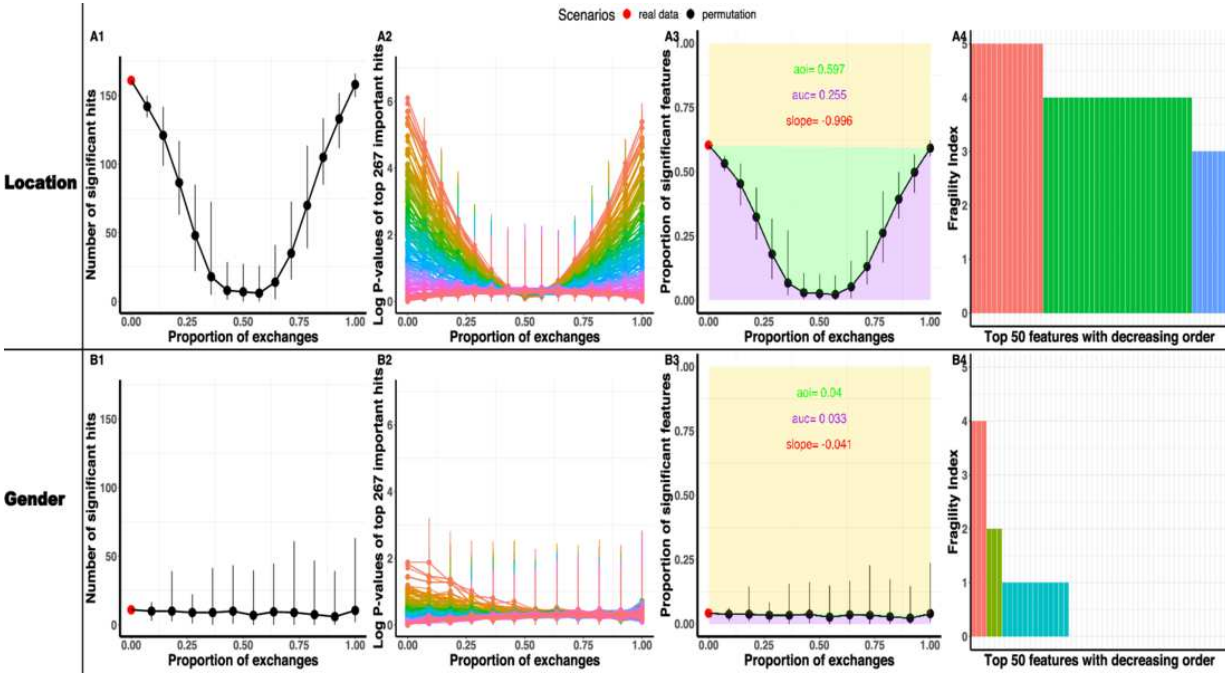


**Fig. 3.** Result comparisons when linking microbiome compositions with location (A1-A4) and gender (B1-B4). A1 and B1 plot the U-Curve of number of significant hits. In A2 and B2, we rank the significance of the 267 features, and then plot their  $-\log_{10} p$ -values with the same order across permutation scenarios. A3 and B3 plot the U-Curve of proportion of significant hits. A4 and B4 plots the fragility index of the top 100 features with a decreasing order. To save space, the legend listing the names of the 100 features are omitted.

in real Data, please see the histograms in Section S2 of Supplementary material.

SimData 1:  $D_{11}$  contains 8 samples. The mean is  $[(6)_{30}, (4)_{30}, (1)_{40}]$ . The dispersion parameter  $\kappa$  is 2.  $D_{12}$  contains 22 samples. The mean is

$[(4)_{30}, (6)_{30}, (1)_{40}]$ . The dispersion parameter  $\kappa$  is 36.  $D_2$  contains 30 samples. The mean is  $[(15)_{30}, (0.5)_{30}, (1)_{40}]$ . The dispersion parameter  $\kappa$  is 36.

SimData2:  $D_{11}$  contains 16 samples. The mean is  $[(8)_{30}, (2)_{30}, (1)_{40}]$ . The dispersion parameter  $\kappa$  is 25.  $D_{12}$  contains 14 samples. The mean is  $[(2)_{30}, (8)_{30}, (1)_{40}]$ . The dispersion parameter  $\kappa$  is 24.  $D_{21}$  contains 20 samples. The mean is  $[(15)_{30}, (0.5)_{30}, (1)_{40}]$ . The dispersion parameter  $\kappa$  is 26.  $D_{22}$  contains 10 samples. The mean is  $[(m_1)_{60}, (m_2)_{40}]$ , where  $m_1 = \text{RN}(5, 1.2)$  and  $m_2 = \text{RN}(1, 0.1)$ . The dispersion parameter  $\kappa$  is 24.

SimData3:  $D_{11}$  contains 24 samples. The mean is  $[(8)_{30}, (2)_{30}, (1)_{40}]$ . The dispersion parameter  $\kappa$  is 14.  $D_{12}$  contains 6 samples. The mean is  $[(1)_{30}, (10)_{30}, (1)_{40}]$ . The dispersion parameter  $\kappa$  is 14.  $D_{21}$  contains 20 samples. The mean is  $[(15)_{30}, (0.5)_{30}, (1)_{40}]$ . The dispersion parameter  $\kappa$  is 14.  $D_{22}$  contains 10 samples. The mean is  $[(m_1)_{60}, (m_2)_{40}]$ , where  $m_1 = \text{RN}(5, 1.6)$  and  $m_2 = \text{RN}(1, 0.3)$ . The dispersion parameter  $\kappa$  is 12.

Based on the above setup, we expect to see there are more and more confounding effects from SimData 1 to SimData 2 to SimData 3. As a result, the associations between the microbiome features and the grouping factor of interest is weaker and weaker because the proportion of differential samples between Group 1 and Group 2 is lower and lower. Traditionally, non-metric multidimensional scaling (NMDS) is used to collapse information from multiple dimensional features into just a few, so that clustering effect will be visualized and interpreted when we link them with a grouping factor of interest (Cox and Cox, 2000). However, in the dimension reduction plots, the expected clustering effect can not be witnessed, because this main differential effect is mixed with heterogeneity. As shown in Fig. 1, only the NMDS plot of SimData 1 shows us the clear cluster separations between Group 1 and Group 2. But both the NMDS plot of SimData 2 and the NMDS plot of SimData 3 show overlaps of Group 1 and Group 2 similarly. Therefore, NMDS plots could not distinguish the strength of the overall association between microbiome compositions and the grouping factor of interest. Besides, we can not visualize differences in confounding effects between simulation 2 and simulation 3.

When testing the relationship between an explanatory variable and an outcome, the variable’s effect might be modified by other variables (known or unknown) and distorted by potential systematic bias, confounding or effect modification. The U-curve and fragility index plots provides us with a measure of all these disturbances mixed with the main signals in the collected data. The U-curve provides a dynamic depiction of how our method progressively singles out signals from randomized trials. In each plot, the number of significant features decreases from real data to full permuted scenario. The shape becomes wider (steeper decline) when the associations are less stable (with more disturbances). We use AUC (area under curve) to quantify the shape of the U-Curve. AUCs in Fig. 1D, E and F are 0.429, 0.298 and 0.186, which ranks the decreasing order of robustness of the association between microbiome compositions and the grouping factor. We define the scale as  $s = 0.75$ , which describes that the maximum AUC is 75% of the current AOI. The overall association is defined as  $OA = \sqrt{\frac{AUC}{s \cdot AOI}}$ . Therefore, the rescaled AUCs become 0.98, 0.81 and 0.64.

Please note that, for permutation scenario  $k$ , there are as many as  $\binom{n_1}{k} \binom{n_2}{k}$  different ways of exchanging the grouping factor labels. Therefore, when doing the U-Curve plots (D, E, F in Fig. 1), the black dots describe the median value. The black bars describe the 2.5% and 97.5% quantile intervals. We follow the same setup in all the subsequent figures.

## 4 Results

In this section, we apply the proposed method into two microbiome studies. The first study includes five groups. We regroup them to construct two

data sets with different levels of heterogeneity. In the second study, we link microbiome compositions with two different outcomes.

The first study examined the gut microbiota of 350 stool samples collected longitudinally for more than a year from the Hadza hunter gatherers of Tanzania. The samples were collected subsequently with 5 seasonal groups: 2013-LD (Late dry), 2014-EW (Early wet), 2014-LW (Late wet), 2014-ED (Early dry) and 2014 LD (Late Dry). Smits *et al.*, 2017 found that Hadza gut microbial community compositions are cyclic and differentiated by season. They observed that samples from the dry seasons were distinguishable from the wet seasons and were indistinguishable from other dry seasons in sequential years. We combine 2014-ED ( $n = 33$ ) and 2014-LD ( $n = 133$ ) as the “Dry” group, and combine 2014-EW ( $n = 62$ ) and 2014-LW ( $n = 58$ ) as the “Wet” group. We call this regrouped data as SmitsData 1. In the same way, we combine 2013-LD ( $n = 64$ ) and 2014-EW ( $n = 62$ ) as the “LDEW” group, and combine 2014-LW ( $n = 58$ ) and 2014-ED ( $n = 33$ ) as the “LWED” group. We call this regrouped data as SmitsData 2. We expect that SmitsData 1 is more differentiated between Dry and Wet group than SmitsData 2 between LDEW and LWED group.

In total, we have 786 taxonomic features. We perform the progressive permutation tests on SmitsData 1 (Dry  $n_1 = 166$  vs. Wet  $n_2 = 120$ ) and SmitsData 2 (LDEW  $n_1 = 126$  vs. LWED  $n_2 = 91$ ). The results of SmitsData 1 (A1-A4) and SmitsData 2 (B1-B4) are shown in Fig. 2. We identify more significant hits ( $p$ -value less than 0.05) from SmitsData 1 (672 in A1) than SmitsData 2 (345 in B1). There are more  $-\log_{10} p$ -values greater than  $-\log_{10} 0.05$  (A2 vs. B2). The U-curve of SmitsData 1 (AUC is 0.53, rescaled as 0.92) is steeper than SmitsData 2 (AUC is 0.148, rescaled as 0.72). Based on the plot of fragility index, the overall robustness of the top 100 features from SmitsData 1 (more than 40 in A4) is more than SmitsData 2 (less than 40 in B4). All these results verify that the progressive permutation results can measure the overall association which is disturbed by heterogeneity.

The second study investigated the impact of diet by comparing the gut microbiota of 14 Children aged 1-6 years in a village of rural Africa with the gut microbiota of 15 European children at the same age. De Filippo *et al.*, 2010 found significant differences in gut microbiota between the two groups, as children at these two locations have different dietary habits. 11 of them are female. 18 of them are male. There is almost no difference in microbiome compositions by gender. In total, we have 267 taxonomic features. We perform the progressive permutation tests to associate microbiome compositions with location and gender respectively. The results of location (A1-A4) and gender (B1-B4) are shown in Fig. 3. The results illustrate that microbiome compositions are strongly associated with location instead of gender, because AUC of location (0.255 in A3, rescaled as 0.75) is greater than AUC of gender (0.033 in B3, no need to rescale). The U-curves of gender (B1 and B3) are almost flat, which imply that the overall association between microbiome compositions and gender is weak.

We include the identification of individual features in our software by observing whether the  $-\log_{10} p$ -values of targeted features lie within the 95% confidence interval of median  $-\log_{10} p$ -values of the full mixing scenario. As shown in the upper left panel in Fig. 4, all the top 50 features are significant. The effect sizes of these 50 significant features are plotted in the upper right panel. Our findings are consistent with published results (De Filippo *et al.*, 2010). Firmicutes are more abundant in European children than in African children. Prevotella and Treponema (Spirochaetaceae) are more abundant in African children than in European children (as shown in the lower panels of Fig. 4).

In summary, our method first explores the overall association (that might be complicated by confounding effect) between microbiome compositions and outcome variable. If the association is reasonable, it

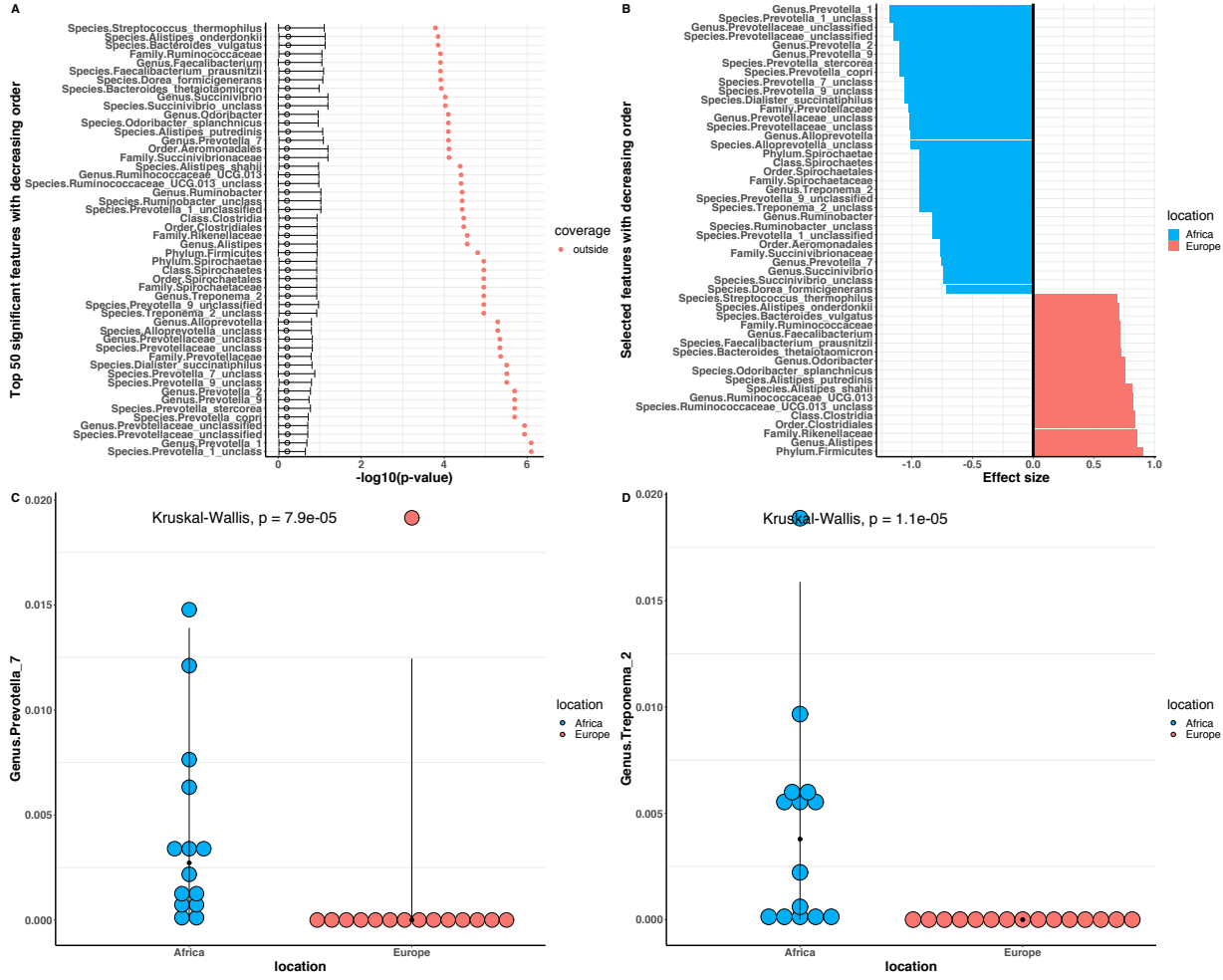


**Fig. 4.** List of discoveries, effect sizes and individual abundances. A denotes the coverage plot of the top 50 features with decreasing order. The color dots denote the  $-\log_{10} p$ -value of top 50 features in the original data (permutation proportion is 0). The horizontal bars describe the 95% quantile confidence intervals of the  $-\log_{10} p$ -value in the full permutation scenario. B denotes the effect sizes of identified features. C and D denote the dot plot of abundance of *Prevotella* and *Treponema* with median-quantile vertical lines.

will identify the significance of individual hits, list their effect sizes and plot individual abundances.

## 5 Analytical function of U-Curve

Various summary statistics, like mean, variances, median and rank sums, have been used to analyze differences between two groups. Each statistic goes along with an assumption of a sample distribution, including normal, negative binomial and so on. Among these, the mean test under a normal assumption is one of the most widely-used statistical techniques for group comparisons. Other types of tests extend the standard to broader situations that require specific assumptions or less restrictions. Therefore, it is worthwhile to pursue the theoretical aspects of the progressive permutation method in a basic setup that performs Z-tests. The theoretical results from parametric tests can provide insights to the progressive permutation coupling non-parametric tests, as we expect to observe similar patterns between them. To simplify the problem, we assume to observe two groups of variables from Gaussian family. We assume that both groups have the same number of variables  $p$ . We use  $x_{ij}^1$  to denote the  $i$ th observation of the  $j$ th variable in group 1 and  $x_{ij}^2$  to denote the  $i$ th observation of the  $j$ th

variable in group 2. We denote the labels in Group 1 as  $I^1 = \{1, \dots, n_1\}$ . We denote the labels in Group 2 as  $I^2 = \{1, \dots, n_2\}$ . We assume that  $x_{ij}^1 \sim \mathcal{N}(\mu_j^1, \sigma)$  and  $x_{ij}^2 \sim \mathcal{N}(\mu_j^2, \sigma)$ , which means that observations of every variable in each group are independent and identically distributed. We aim to test the hypothesis  $H_{0j} : \mu_j^1 = \mu_j^2$ , vs.  $H_{1j} : \mu_j^1 \neq \mu_j^2$ . To test the difference of the  $j$ th variable between the two groups of the original data, we calculate the mean difference between the two groups,

$$\bar{x}_j^1 - \bar{x}_j^2 = \frac{1}{n_1} \sum_{i=1}^{n_1} x_{ij}^1 - \frac{1}{n_2} \sum_{i=1}^{n_2} x_{ij}^2 \sim \mathcal{N}(\mu_j^1 - \mu_j^2, \frac{n_1 + n_2}{n_1 n_2} \sigma^2). \quad (1)$$

Suppose we perform the progressive permutation method and randomly draw  $k$  samples from group 1 and  $k$  samples from group 2, and then exchange their grouping labels. We denote the selected labels in Group 1 as  $I_k^1 = \{i_1^1, \dots, i_k^1\}$ . We denote the selected labels in Group 2 as  $I_k^2 = \{i_1^2, \dots, i_k^2\}$ . Then the mean difference of the  $j$ th variable between



the two groups of permutation scenario  $k$  becomes

$$\begin{aligned} \bar{x}_j^1 - \bar{x}_j^2 &= \frac{1}{n_1} \sum_{i \in I^1 \setminus I_k^1} x_{ij}^1 + \frac{1}{n_1} \sum_{i \in I_k^2} x_{ij}^2 \\ &\quad - \frac{1}{n_2} \sum_{i \in I^2 \setminus I_k^2} x_{ij}^2 - \frac{1}{n_2} \sum_{i \in I_k^1} x_{ij}^1 \\ &\sim \mathcal{N} \left( \left(1 - \frac{n_1 + n_2}{n_1 n_2} k\right) (\mu_1 - \mu_2), \frac{n_1 + n_2}{n_1 n_2} \sigma^2 \right). \end{aligned} \quad (2)$$

The mean differences in tests after permutation (2) are smaller than those in tests before permutation (1). Suppose  $\frac{\mu_j^1 - \mu_j^2}{\sigma} = \delta_j$  and  $\mu_j^1 > \mu_j^2$ . Then the p-value of the  $j$ th variable is

$$\begin{aligned} p_j(k) &= P \left( |z| > \frac{\bar{x}_j^1 - \bar{x}_j^2}{\sqrt{\frac{n_1 + n_2}{n_1 n_2} \sigma^2}} \right) \\ &= 2\Phi \left( -\sqrt{\frac{n_1 n_2}{2(n_1 + n_2)}} \left(1 - \frac{n_1 + n_2}{n_1 n_2} k\right) \delta_j \right), \end{aligned} \quad (3)$$

where  $k \leq \frac{n_1 n_2}{n_1 + n_2}$ .  $\Phi(\cdot)$  denotes the cumulative function of standard normal distribution. Therefore, with the increase of exchanged labels  $k$ ,  $-\log_{10} p$ -value is smaller. As we perform two sided Z-tests in each scenario, the permutation results (p-values) are symmetric with respect to the fully mixing scenario  $K_f = \frac{n_1 n_2}{n_1 + n_2}$ . Then we can obtain the p-value of the  $j$ th variable when  $k = K_f, \dots, K$  as  $p_j(k) = 2\Phi \left( \sqrt{\frac{n_1 n_2}{2(n_1 + n_2)}} \left(1 - \frac{n_1 + n_2}{n_1 n_2} k\right) \delta_j \right)$ .  $-\log_{10} p_j(k)$  decreases with  $k$  when  $0 \leq k \leq K_f$  and increases with  $k$  when  $K_f \leq k \leq K$ . We define  $\frac{k}{K}$  as the proportion of permutations. We let  $n_1 = n_2 = 20$ . Then we observe in Fig.5,  $-\log_{10} p_j(k)$  is a U-Curve of  $\frac{k}{K}$ . If the mean difference of the variable is bigger, the U-Curve is steeper. If the standard deviation of the variable is bigger, the U-Curve is flatter. Therefore, the steepness of the U-Curve measures how differential the quantifies of interest are between the two groups.

## 6 Discussion

The proposed method considers the signal identification problem as progressively singling out signals from permuted randomized versions of an original data set. It progressively permutes the grouping factor of the microbiome data and performs multiple differential abundance tests in each scenario. We then summarize the resulting p-values by the number of significant hits and calculate their fragility index to quantify the overall association with the grouping factor and robustness of the discovered microbes. Based on these global characteristics, we can judge whether to identify the significance of individual hits. We achieve this by comparing the p-values of the original data with p-values of the full permuted data. We have developed these methods into a user-friendly and efficient R-shiny tools with visualizations.

Our proposed method will present a steeper U-curve when the overall association with grouping factor is strong. Furthermore, it can quantify different levels of heterogeneity which is a common phenomenon in medical research. The associations between microbiome compositions and a grouping factor may be weak due to a variety of reasons, such as systematic bias, confounding and effect modification. Therefore, we generate three simulated data sets with different levels of heterogeneity. The AUC and fragility index provide a summary of the progressive permutation results to quantify and differentiate heterogeneity. In addition, the application into Smits data and DeFilippo data continue to prove that our proposed method can evaluate the overall association between

microbiome compositions and outcome of interest, rank the robustness of the discovered microbes and identify significant individuals.

In this paper, we link microbiome composition with a binary outcome. It creates a new concept and framework to understand significance and robustness of identified microbiome features. Following the same logic, we can extend the binary outcome to a continuous outcome. When constructing the progressive permutation scenarios, we permute a proportion (select  $k$  samples and calculate  $\frac{k}{n}$ ) of the continuous outcome. In each scenario, we perform the Kendall's Tau and Spearman's Rank Correlation tests to associate microbiome compositions with the permuted continuous outcome. We then adopt similar procedures of the binary outcome to summarize the permutation results. We have applied the progressive permutation with a continuous outcome to a sample data set. Please see the results in Section S3 of the Supplementary material.

Our method does not calculate adjusted p-values. In the future, we will consider to use progressive permutation results to estimate the null distribution to correct false positive rates, so we can adjust the existing p-values according to the null distribution and identify significant hits based on the adjusted p-values.

## Acknowledgements

The authors thank Professor J. Jack Lee for providing us great suggestions on simulations, Norris Clift for helping us launch the Shiny App on the server <https://biostatistics.mdanderson.org/shinyapps/ProgPerm>.

## Funding

KAD is partially supported by MD Anderson Moon Shot Programs, Prostate Cancer SPORE P50CA140388, NIH/NCI CCSG grant P30CA016672, CCTS 5UL1TR000371, and CPRIT RP160693 grants. CBP is partially supported by NIH/NCI CCSG grant P30CA016672 and MD Anderson Moon Shot Programs. RRJ is partially supported by NIH R01 HL124112 and CPRIT RR160089 grants.

## References

- Cani, P. D. and Jordan, B. F. (2018). Gut microbiota-mediated inflammation in obesity: a link with gastrointestinal cancer. *Nature Reviews Gastroenterology & Hepatology*, page 1.
- Cox, T. F. and Cox, M. A. (2000). *Multidimensional scaling*. Chapman and hall/CRC.
- De Filippo, C., Cavalieri, D., Di Paola, M., Ramazzotti, M., Poullet, J. B., Massart, S., Collini, S., Pieraccini, G., and Lionetti, P. (2010). Impact of diet in shaping gut microbiota revealed by a comparative study in children from europe and rural africa. *Proceedings of the National Academy of Sciences*, **107**(33), 14691–14696.
- Feinstein, A. R. (1990). The unit fragility index: an additional appraisal of “statistical significance” for a contrast of two proportions. *Journal of clinical epidemiology*, **43**(2), 201–209.
- Fernandes, A. D., Reid, J. N., Macklaim, J. M., McMurrough, T. A., Edgell, D. R., and Gloor, G. B. (2014). Unifying the analysis of high-throughput sequencing datasets: characterizing rna-seq, 16s rna gene sequencing and selective growth experiments by compositional data analysis. *Microbiome*, **2**(1), 15.
- Goeman, J. J. and Solari, A. (2014). Multiple hypothesis testing in genomics. *Statistics in medicine*, **33**(11), 1946–1978.
- Gopalakrishnan, V., Helmink, B. A., Spencer, C. N., Reuben, A., and Wargo, J. A. (2018). The influence of the gut microbiome on cancer, immunity, and cancer immunotherapy. *Cancer cell*, **33**(4), 570–580.

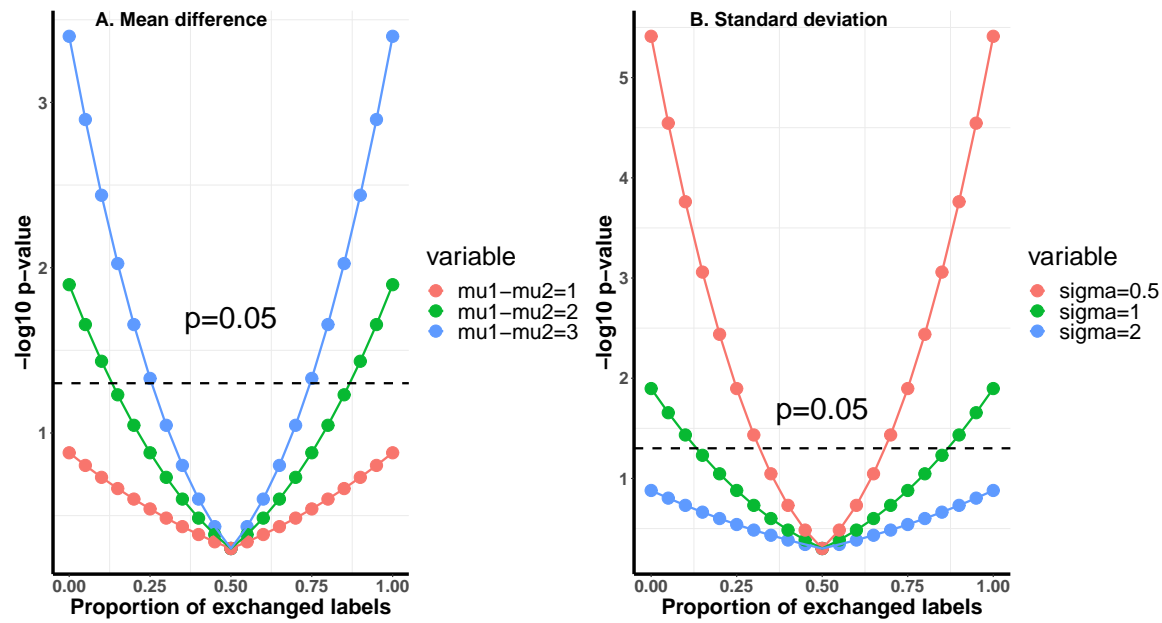


**Fig. 5.** U-Curve plots of p-values calculated from formula 3. Both of the sample sizes  $n_1$  and  $n_2$  are 20. x-axis is  $\frac{k}{K}$ . In panel A, standard deviation  $\sigma$  is fixed at 2. In panel B, mean difference  $\mu_1 - \mu_2$  is fixed at 1.

- Hawinkel, S., Mattiello, F., Bijmens, L., and Thas, O. (2019). A broken promise: microbiome differential abundance methods do not control the false discovery rate. *Briefings in bioinformatics*, **20**(1), 210–221.
- Jiang, L., Amir, A., Morton, J. T., Heller, R., Arias-Castro, E., and Knight, R. (2017). Discrete false-discovery rate improves identification of differentially abundant microbes. *MSystems*, **2**(6), e00092–17.
- Jie, Z., Xia, H., Zhong, S.-L., Feng, Q., Li, S., Liang, S., Zhong, H., Liu, Z., Gao, Y., Zhao, H., et al. (2017). The gut microbiome in atherosclerotic cardiovascular disease. *Nature communications*, **8**(1), 845.
- Knight, R., Vrbanc, A., Taylor, B. C., Aksenov, A., Callewaert, C., Debelius, J., Gonzalez, A., Kosciolek, T., McCall, L.-I., McDonald, D., et al. (2018). Best practices for analysing microbiomes. *Nature Reviews Microbiology*, **16**(7), 410.
- Love, M. I., Huber, W., and Anders, S. (2014). Moderated estimation of fold change and dispersion for rna-seq data with deseq2. *Genome biology*, **15**(12), 550.
- Mandal, S., Van Treuren, W., White, R. A., Eggesbø, M., Knight, R., and Peddada, S. D. (2015). Analysis of composition of microbiomes: a novel method for studying microbial composition. *Microbial ecology in health and disease*, **26**(1), 27663.
- Ong, I. M., Gonzalez, J. G., McIlwain, S. J., Sawin, E. A., Schoen, A. J., Adluru, N., Alexander, A. L., and John-Paul, J. Y. (2018). Gut microbiome populations are associated with structure-specific changes in white matter architecture. *Translational psychiatry*, **8**(1), 6.
- Owen, A. B. (2013). *Monte Carlo theory, methods and examples*.
- Paulson, J. N., Stine, O. C., Bravo, H. C., and Pop, M. (2013). Differential abundance analysis for microbial marker-gene surveys. *Nature methods*, **10**(12), 1200.
- Riquelme, E., Zhang, Y., Zhang, L., Montiel, M., Zoltan, M., Dong, W., Quesada, P., Sahin, I., Chandra, V., San Lucas, A., et al. (2019). Tumor microbiome diversity and composition influence pancreatic cancer outcomes. *Cell*, **178**(4), 795–806.
- Robinson, M. D., McCarthy, D. J., and Smyth, G. K. (2010). edgeR: a bioconductor package for differential expression analysis of digital gene expression data. *Bioinformatics*, **26**(1), 139–140.
- Segata, N., Izard, J., Waldron, L., Gevers, D., Miropolsky, L., Garrett, W. S., and Huttenhower, C. (2011). Metagenomic biomarker discovery and explanation. *Genome biology*, **12**(6), R60.
- Smirnova, E., Huzurbazar, S., and Jafari, F. (2019). Perfect: Permutation filtering test for microbiome data. *Biostatistics*, **20**(4), 615–631.
- Smits, S. A., Leach, J., Sonnenburg, E. D., Gonzalez, C. G., Lichtman, J. S., Reid, G., Knight, R., Manjurano, A., Chagalucha, J., Elias, J. E., et al. (2017). Seasonal cycling in the gut microbiome of the hadza hunter-gatherers of tanzania. *Science*, **357**(6353), 802–806.
- Vogt, N. M., Kerby, R. L., Dill-McFarland, K. A., Harding, S. J., Merluzzi, A. P., Johnson, S. C., Carlsson, C. M., Asthana, S., Zetterberg, H., Blennow, K., et al. (2017). Gut microbiome alterations in Alzheimer’s disease. *Scientific reports*, **7**(1), 13537.
- Walsh, M., Srinathan, S. K., McAuley, D. F., Mrkobrada, M., Levine, O., Ribic, C., Molnar, A. O., Dattani, N. D., Burke, A., Guyatt, G., et al. (2014). The statistical significance of randomized controlled trial results is frequently fragile: a case for a fragility index. *Journal of clinical epidemiology*, **67**(6), 622–628.
- Wei, X., Tao, J., Xiao, S., Jiang, S., Shang, E., Zhu, Z., Qian, D., and Duan, J. (2018). Xiexin tang improves the symptom of type 2 diabetic rats by modulation of the gut microbiota. *Scientific reports*, **8**(1), 3685.